Carcinogenesis vol.28 no.1 pp.163–173, 2007
doi:10.1093/carcin/bgl145
Advance Access publication August 18, 2006

Pomegranate fruit extract inhibits prosurvival pathways in human A549 lung carcinoma cells and tumor growth in athymic nude mice

Naghma Khan, Naghma Hadi, Farrukh Afaq, Deeba N.Syed, Mee-Hyang Kweon and Hasan Mukhtar*

Department of Dermatology, University of Wisconsin, Madison, WI 53706, USA

*To whom correspondence should be addressed. Helfaer Professor of Cancer Research, Director and Vice Chair of Research, Department of Dermatology, University of Wisconsin-Madison, 1300, University Avenue, Medical Sciences Center, B-25, Madison, WI 53706, USA. Tel: +1 608 263 3927; Fax: +1 608 263 5223;
Email: hmukhtar@wisc.edu

Developing novel mechanism-based chemopreventive approaches for lung cancer through the use of dietary substances which humans can accept has become an important goal. In the present study, employing normal human bronchial epithelial cells (NHBE) and human lung carcinoma A549 cells, we first compared the growth inhibitory effects of pomegranate fruit extract (PFE). Treatment of PFE (50–150 μg/ml) for 72 h was found to result in a decrease in the viability of A549 cells but had only minimal effects on NHBE cells as assessed by the MTT and Trypan blue assays. PFE treatment of A549 cells also resulted in dose-dependent arrest of cells in G_0–G_1 phase of the cell cycle (as assessed by DNA cell cycle analysis). We further found that PFE treatment also resulted in (i) induction of WAF1/p21 and KIP1/p27, (ii) decrease in the protein expressions of cyclins D1, D2 and E, and (iii) decrease in cyclin-dependent kinase (cdk) 2, cdk4 and cdk6 expression. The treatment of cells with PFE inhibited (i) phosphorylation of MAPK proteins, (ii) inhibition of PI3K, (iii) phosphorylation of Akt at Thr^{308}, (iv) NF-κB and IKKα, (v) degradation and phosphorylation of IκBα, and (vi) Ki-67 and PCNA. We also found that PFE treatment to A549 cells resulted in inhibition of NF-κB DNA-binding activity. Oral administration of PFE (0.1 and 0.2%, wt/vol) to athymic nude mice implanted with A549 cells resulted in a significant inhibition in tumor growth. Our results provide a suggestion that PFE can be a useful chemopreventive/chemotherapeutic agent against human lung cancer.

Introduction

Lung cancer as the most common cancer in the world represents a major public health problem (1). Worldwide it accounts for ∼1.18 million cancer-related deaths and is the most common cause of cancer death in both men and women. Tobacco smoking is well established as the major etiological risk factor for lung cancer, contributing to a 10-fold increase in risk in long-term smokers compared with non-smokers. Other environmental risk factors include exposure to radiation, asbestos, heavy metals (arsenic, chromium and nickel), polycyclic aromatic hydrocarbons and chloromethyl ethers (2,3). Despite major advances in the treatment and management of lung cancer, most patients with lung cancer eventually die of this disease. Because conventional therapies have failed to make a major impact on survival, newer approaches are necessary in the battle against lung cancer. The poor lung cancer survival figures argue powerfully for new approaches to control this disease through chemoprevention, which has been defined as the use of agents that could reverse, suppress or completely halt tumor development.

Pomegranate (*Punica granatum*, Punicaceae), is an edible fruit cultivated in Mediterranean countries, Afghanistan, India, China, Japan, Russia and the United States. Edible parts of pomegranate fruit (∼80% of total fruit weight) comprise 80% juice and 20% seed. Pomegranate is a rich source of crude fibers, pectin, sugars and several tannins, its juice and seed oil contains certain species of flavonoids and anthocyanins which provide the fruit potent antioxidant activity. Recently, pomegranate juice was found to revert the potent down regulation of the expression of endothelial nitric oxide synthase induced by oxidized low-density lipoprotein in human coronary endothelial cells (4). Dietary supplementation of polyphenol-rich pomegranate juice to atherosclerotic mice was shown to inhibit significantly the development of atherosclerotic lesions (5). It has also been shown that pomegranate can suppress NF-κB activation through a novel mechanism in vascular endothelial cells (6). We extracted edible seeds of pomegranate fruit with acetone, hereafter referred to as pomegranate fruit extract (PFE). Based on matrix-assisted laser desorption/ionization time-of-flight mass spectrometry (MALDI-TOF MS) analysis, PFE was found to contain anthocyanins (such as delphinidin, cyanidin and pelargonidin) and hydrolyzable tannins (such as punicalin, pedunculagin, punicalagin, gallagic and ellagic acid esters of glucose). The hydrolyzable tannins account for 92% of the antioxidant activity of the whole fruit (7). Recent work from our laboratory shows that PFE possesses remarkable antitumor promoting effects in mouse skin (8) and antiproliferative and proapoptotic effects in prostate cancer (9). We have also shown that PFE protects against the adverse effects of UV-B and UV-A radiation by inhibiting cellular pathways in normal human epidermal kerationocytes (10,11).

We hypothesized that PFE may afford chemopreventive as well as cancer-chemotherapeutic effects against lung cancer. In this study, we first demonstrated the antiproliferative effects of PFE in A549 cells. This involves the arrest of cells in G_1 phase of the cell cycle and involvement of *cki-cyclin-cdk* network. Next, we determined the chemopreventive potential of PFE on phosphorylation and activation of MAPK, NF-κB, PI3K/Akt pathways in A549 human lung carcinoma cells. Based on the results of our *in vitro* data, we next carried out *in vivo* study in mice. We found that oral

Abbrevations: MAPK, mitogen-activated protein kinase; NF-κB, nuclear factor kappa B; PFE, pomegranate fruit extract.

administration of a human acceptable dose of PFE to athymic nude mice implanted with A549 cells resulted in significant inhibition of tumor growth.

Materials and methods

Materials

ERK1/2 (phospho-p44/42, Thr202/Tyr204), JNK (phospo-p54/46, Thr183/Tyr185), p38 (phospho-p38, Thr180/Tyr204), IκBα, IκBα (phospho), anti-cyclins D1, D2 and E antibodies were obtained from Cell Signaling Technology (Beverly, MA, USA). The mono and polyclonal antibodies IKKα, cdks 2, 4 and 6, WAF1/p21 and KIP1/p27 were obtained from Santa Cruz Biotechnology Inc. (Santa Cruz, CA, USA). NF-κB/p65, phospho-Akt (Thr 308), PI3K (p85 and p110) were procured from Upstate (Lake Placid, NY, USA). Anti-mouse and anti-rabbit secondary antibody horseradish peroxidase (HRP) conjugate was obtained from Amersham Life Science Inc. (Arlington Height, IL, USA). Lightshift™ chemiluminescent EMSA kit and BCA Protein assay kit were obtained from Pierce (Rockford, IL, USA). ELISA kit was purchased from Active Motif (CA, USA). Novex precast Tris–glycine gels were obtained from Invitrogen (Carlsbad, CA, USA). The Apo-Direct kit for flow cytometry was purchased from Phoenix Flow Systems (San Diego, CA, USA). Trolox antioxidant assay kit was purchased from Cayman chemical (Ann Arbor, MI, USA).

Preparation of PFE

Fresh fruit of pomegranate was peeled, and its edible portion (seed coat and juice) was squeezed in 70% acetone/30% distilled water (1:20, by v/v). The red extract was filtered through filter paper (Whatman no. 1). The filtrate was condensed and freeze dried. The freeze-dried extract was stored at 4°C to be used for various treatments. In our recent publication we have analyzed the PFE employing a novel technique of Matrix Assisted Laser Ionization Time of Flight Mass Spectrometry (MALDI-TOF MS). The PFE preparation used in this study was found to contain six anthocyanins (pelargonidin 3-glucoside, cyanidine 3-glucoside, delphinidin 3-glucoside, pelargonidin 3,5-diglucoside, cyanidine 3,5-diglucoside and delphinidin 3,5-diglucoside), ellagitannins and hydrolysable tannins (8).

Cell culture and treatment

The human lung carcinoma A549 cells were obtained from American Type Culture Collection (ATCC; Manassas, VA, USA) and cultured in F12K medium (ATCC), supplemented with 10% fetal bovine serum, 1% penicillin/streptomycin (P-S) in a 5% CO_2 atmosphere at 37°C. Normal human bronchial epithelial cells (NHBE) were obtained from Clonetics Airway Epithelial Cell Systems (Cambrex Bio Science, Walkersville, Inc., USA) and cultured in bronchial epithelial growth media supplemented with growth factors (Cambrex Bio Science). PFE was dissolved in dimethyl sulfoxide (DMSO) and was used for the treatment of cells. A total of 50–60% confluent cells were treated with PFE (50–150 μg/ml) for 72 h in complete growth medium.

Cell viability

The effect of PFE on the viability of cells was determined by 3-[4,5-dimethylthiazol-2-yl]-2,5-diphenyl tetrazoliumbromide assay. The cells were plated at 1×10^4 cells/well in 200 μl of complete culture medium containing 50–150 μg/ml concentrations of PFE in 96-well microtiter plates for 72 h. After incubation for specified times at 37°C in a humidified incubator, 3-[4,5-dimethylthiazol-2-yl]-2,5-diphenyl tetrazoliumbromide (5 mg/ml in PBS) was added to each well and incubated for 2 h, after which the plate was centrifuged at 1800× *g* for 5 min at 4°C. The absorbance was recorded on a microplate reader at the wavelength of 540 nm. The effect of PFE on growth inhibition was assessed as percent cell viability where DMSO-treated cells were taken as 100% viable. DMSO at the concentrations used was without any effect on cell viability.

Measurement of antioxidant activity

To assess the antioxidant capacity of PFE in A549 cells, trolox antioxidant assay was performed using the trolox antioxidant assay kit from Cayman chemical following the vendor's protocol. The total reaction volume of 210 μl consisted of 10 μl of trolox standard (A–G), 10 μl of metmyoglobin and 150 μl of reconstituted chromogen per well in the designated standard wells on the 96-well plate. The sample wells consisted of 30 μg cell lysate, 10 μl of metmyoglobin and 150 μl of reconstituted chromogen. The final volume of 210 μl was adjusted in the sample wells with the assay buffer provided in the kit. All samples were assayed in duplicate. The reaction was initiated by adding 40 μl of hydrogen peroxide working solution (441 μM) to all the wells being used. The plate was covered and incubated at room temperature for 5 min and absorbance was read at 750 nm using a plate reader.

DNA cell cycle analysis

The cells (50–60% confluent) were treated with PFE (50–150 μg/ml) for 72 h in complete medium. The cells were trypsinized thereafter, washed twice with cold PBS and centrifuged. The cell pellet was resuspended in 50 μl cold PBS to which cold methanol (450 μl) was added and the cells were incubated for 1 h at 4°C. The cells were centrifuged at 1100 r.p.m. for 5 min, pellet washed twice with cold PBS, suspended in 500 μl PBS and incubated with 5 μl RNase (20 μg/ml final concentration) for 30 min. The cells were chilled over ice for 10 min and incubated with propidium iodide (50 μg/ml final concentration) for 1 h for analysis by flow cytometry. Flow cytometry was performed with a FACScan (Becton Dickinson, Germany). A minimum of 10 000 cells/sample were collected and the DNA histograms were further analyzed by using ModiFitLT software (Verily Software House, Topsham, ME, USA) for cell cycle analysis.

Preparation of cytosolic and nuclear lysates

Following treatment of cells with PFE, the medium was aspirated and the cells were washed twice in PBS (10 mM, pH 7.4). The cells were incubated in 0.4 ml ice-cold lysis buffer (HEPES (10 mM, pH 7.9), KCl (10 mM), EDTA (0.1 mM), EGTA (0.1 mM), DTT (1 mM), PMSF (1 mM) with freshly added protease inhibitor cocktail (Protease Inhibitor Cocktail Set III; Calbiochem, La Jolla, CA, USA) for 15 min, after which 12.5 μl of 10% Nonidet P-40 was added and the contents were mixed on a vortex and then centrifuged for 1 min (14 000× *g*) at 4°C. The supernatant was saved as cytosolic lysate and stored at −80°C. The nuclear pellet was resuspended in 50 μl of ice-cold nuclear extraction buffer [HEPES (20 mM, pH 7.9), NaCl (0.4 M), EDTA (1 mM), EGTA (1 mM), DTT (1 mM), PMSF (1 mM)] with freshly added protease inhibitor cocktail (Protease Inhibitor Cocktail Set III; Calbiochem) for 30 min with intermittent mixing. The tubes were centrifuged for 5 min (14 000× *g*) at 4°C, and the supernatant (nuclear extract) was stored at −80°C. The protein concentration was determined by the BCA Protein assay kit obtained from Pierce.

Enzyme-linked immunosorbent assay

The commercially available Trans-AM kit (Active Motif) that was employed for the assay of NF-κB/p65 uses an oligonucleotide containing an NF-κB consensus site (5′-GGGACTTTCC-3′) that binds to the nuclear extract and can detect NF-κB, which can recognize an epitope on p65 activated and bound to its target DNA. In the absence of competitive binding with the wild-type or mutated consensus oligonucleotide, 30 μl of binding buffer was added to each well in duplicate. Alternatively, 30 μl of binding buffer containing 20 pmol (2 μl) of appropriate oligonucleotide, in duplicate, was added to the corresponding well. Nuclear lysate protein (5 μg) of each sample diluted in 20 μl lysis buffer was loaded per well. The plate was sealed with the adhesive film and incubated for 1 h at room temperature with mild agitation (100 r.p.m. on a rocking platform), after which the well was washed three times with 200 μl of 1× wash buffer and 100 μl of diluted primary antibody (1:1000 dilution in 1× antibody-binding buffer) was added to each well and incubated at room temperature for 1 h without agitation. The wells were washed again three times with 1× wash buffer, and 100 μl of diluted HRP conjugate antibody (1:1000 dilution in 1× antibody-binding buffer) was added to each well and incubated for 1 h. The wells were again washed four times with 1× wash buffer followed by the addition of 100 μl of developing solution. The content was incubated for 5 min at room temperature. This was followed by addition of 100 μl of stop solution to each well and the absorbance was read within 5 min at 450 nm.

Electrophoretic mobility shift assay

Electrophoretic mobility shift assay (EMSA) for NF-κB was performed using a lightshift™ chemiluminescent EMSA kit (Pierce) by following the manufacturer's protocol. To start with, DNA was biotin labeled using the Biotin 3′ endlabeling kit (Pierce). Briefly, in a 50 μl reaction buffer, 5 pmol of double-stranded NF-κB oligonucleotide 5′-AGT TGA GGG GAC TTT CCC AGG C-3′; 3′-TCA ACT CCC CTG AAA GGG TCC G-5′ was incubated in a microfuge tube with 10 μl of 5× terminal deoxynucleotidyl transferase (TdT) buffer, 5 μl of 5 M biotin-N4-CTP, 10 U of diluted TdT, and 25 μl of ultrapure water and incubated at 37°C for 30 min. The reaction was stopped with 2.5 μl of 0.2 M EDTA. To extract labeled DNA, 50 μl of chloroform: isoamyl alcohol (24:1) was added to each tube and centrifuged briefly at 13 000× *g*. The top aqueous phase containing the labeled DNA was removed and saved for binding reactions. Each binding reaction contained 1× binding buffer (100 mM Tris, 500 mM KCl, 10 mM dithiothreitol, pH 7.5), 2.5% glycerol, 5 mM $MgCl_2$, 50 ng/μl poly (dI-dC), 0.05% NP-40, 5 μg of nuclear extract and 20–50 fm of biotin-endlabeled target DNA. The

content was incubated at room temperature for 20 min. To this reaction mixture, 5 µl of 5× loading buffer was added, subjected to gel electrophoresis on a native polyacrylamide gel, and transferred to a nylon membrane. When the transfer was complete, DNA was crosslinked to the membrane at 120 mJ/cm^2 using a UV crosslinker equipped with 254 nm bulbs. The biotin-endlabeled DNA was detected using streptavidin–HRP conjugate and a chemiluminescent substrate. The membrane was exposed to X-ray film (XAR-5 Amersham Life Science Inc.) and developed using a Kodak film processor.

Protein extraction and western blotting

Following the treatment of cells as described above, the media was aspirated, the cells were washed with cold PBS (pH 7.4), and ice-cold lysis buffer (50 mM Tris–HCl, 150 mM NaCl, 1 mM EGTA, 1 mM EDTA, 20 mM NaF, 100 mM Na_3VO_4, 0.5% NP-40, 1%Triton X-100, 1 mM PMSF (pH 7.4) with freshly added protease inhibitor cocktail (Protease Inhibitor Cocktail Set III; Calbiochem) over ice for 30 min. The cells were scraped and the lysate was collected in a microfuge tube and passed through needle to break up the cell aggregates. The lysate was cleared by centrifugation at 14?000× *g* for 15 min at 4°C and the supernatant (whole cell lysate) was used or immediately stored at −80°C.

For western blotting, 30–50 µg protein was resolved over 8–12% polyacrylamide gels and transferred to a nitrocellulose membrane. The blot was blocked in blocking buffer (5% non-fat dry milk/1% Tween 20; in 20 mM TBS, pH 7.6) for 1 h at room temperature, incubated with appropriate monoclonal or polyclonal primary antibody in blocking buffer for 1.5 hours to overnight at 4°C, followed by incubation with anti-mouse or anti-rabbit secondary antibody HRP conjugate obtained from Amersham Life Science Inc. and detected by chemiluminescence and autoradiography using XAR-5 film obtained from Eastman Kodak Co. (Rochester, NY, USA). Densitometric measurements of the band in western blot analysis were performed using digitalized scientific software program UN-SCAN-IT (Silk Scientific Corporation, Orem, UT, USA).

Immunocytochemical staining of Ki-67

A549 cells were grown in two chamber tissue culture glass slides. At 50–60% confluence, cells were treated with PFE (50–150 µg/ml) for 72 h and 30 min later cells were fixed in cold methanol (−20°C) for 10 min. Briefly, cells were incubated with TBST (50 mM Tris–HCl; 150 mM NaCl; 0.1% Triton X-100, pH 7.4) for 10 min and then cells were washed with TBS. Five percent goat serum in TBS (50 mM Tris–HCl; 150 mM NaCl, pH 7.4) was added to prevent non-specific antibody binding. The cells were incubated with anti-human Ki-67 (diluted 1:50 in 10% goat serum) overnight at 4°C followed by application of secondary anti-rabbit IgG antibody HRP conjugate (Amersham Biosciences Inc.) for 1 h. Immunoreactions were visualized with DAB as substrate after counterstaining with eosin. Simultaneously, each slide was incubated with isotype control (IgG_1) for an internal negative control. Slides were visualized on a Zeiss Axiophot DM HT microscope. Images were captured with an attached camera linked to a computer. Images and figures were composed by using ADOBE PHOTOSHOP 7.0 (Adobe Systems, Mountain View, CA, USA).

Immunocytochemical staining of NF-κB/p65

A549 cells were seeded in two chamber tissue culture glass slides and treated with PFE (50–150 µg/ml) for 72 h. After treatment, cells were washed with 1× PBS and fixed in 2% paraformaldehyde/1× PBS for 10 min at room temperature. Cells were then permeabilized in cold methanol (−20°C), washed three times with 1× PBS and blocked with 2% donkey (1× PBS) serum for 1 h and incubated with NFκB/p65 antibody [(1:50 in 5% donkey serum (1× PBS)] overnight at 4°C. After three washes with 2% donkey (1× PBS) serum, cells were incubated with donkey anti-rabbit Rhodamine Red ™-X-conjugated antibody [1:50] for 45 min at room temperature. After rinsing in three changes of 2% donkey (1× PBS) serum, samples were mounted using Prolong antifade kit (Invitrogen, Eugene, OR, USA), and observed using a Zeiss Axiophot DM HT microscope. Images were captured with an attached camera linked to a computer. Images and figures were composed using ADOBE PHOTOSHOP 7.0 (Adobe Systems).

In vivo tumor xenograft model

Athymic (*nu/nu*) male nude mice were obtained from NxGen Biosciences (San Diego), housed under pathogen-free conditions with a 12 h light/12 h dark schedule, and fed with an autoclaved diet *ad libitum*. A549 cells were harvested by trypsinization and resuspended in F12K medium. To establish A549 tumor xenografts in mice, 6–8-week-old athymic mice were injected s.c. with 1×10^6 cells mixed with 50 µl of A549 plus 50 µl of Matrigel (Collaborative Biomedical Products, Bedford, MA, USA). Twenty-four animals were then randomly divided into three groups consisting of eight animals each. The first group of animals received normal drinking water and served as controls. The animals of Groups 2 and 3 received the same drinking water supplemented with 0.1% and 0.2% PFE (wt/vol), respectively. Water bottles were changed every other day. The 0.1% and 0.2% doses of PFE selected for feeding mice are based on the assumption that a typical healthy individual (70 kg) may be persuaded to drink 250 or 500 ml of pomegranate juice extracted from one or two fruits, respectively. Body weight, diet and water consumption were recorded twice weekly throughout the study. Tumor sizes were measured twice weekly, and tumor volume was calculated by the formula $0.5238 \times L_1 \times L_2 \times H$ where L_1 is the long diameter, L_2 is the short diameter and H is the height of the tumor (12).

Statistical analysis

Results were analyzed using a two-tailed Student's *t*-test to assess statistical significance and *P*-values <0.05 were considered significant. The Kaplan–Meier method was used to estimate survival, and differences were analyzed by the log-rank test.

Results

Inhibition of cell growth by PFE in A549 but not in NHBE cells

Initially in our study, we investigated the antiproliferative effects of PFE treatment on human lung carcinoma A549 cells. Therefore, using A549 cells, we first evaluated the effect of PFE on the growth of these cells by 3-[4,5-dimethylthiazol-2-yl]-2,5-diphenyl tetrazoliumbromide assay. We compared the antiproliferative effects of PFE on A549 and NHBE cells. As shown in Figure 1A, PFE treatment of A549 cells resulted in 33, 40 and 47% decrease in cell viability at the doses of 50–150 µg/ml of PFE, respectively, but had minimal effect on NHBE cells at these doses. The dose-dependent growth inhibitory effect on A549 cells was also confirmed by Trypan blue exclusion assay as shown in Figure 1B, which also showed a similar growth inhibitory pattern.

Antioxidant capacity of PFE as measured by trolox equivalent antioxidant capacity assay

Trolox is a water-soluble vitamin E derivative commonly used as an antioxidant standard. The higher the trolox equivalent antioxidant capacity (TEAC) value of the sample, the stronger its potential antioxidant activity. PFE caused dose-dependent increase in the $ABTS^+$ scavenging activity in human lung carcinoma A549 cells. As shown in Figure 1C, PFE caused 132, 230 and 238% increase in the TEAC value as compared with the control group.

G_1 phase cell cycle arrest by PFE in A549 cells

To investigate whether PFE treatment has an effect on the cell cycle regulation, we determined its effect on cell cycle distribution by flow cytometry after staining with propidium iodide. As shown in Figure 2, concomitant with growth inhibitory effects, PFE treatment induced a strong G_1 phase cell cycle arrest in a dose-dependent manner. In A549 cells, G_1 phase cell cycle distribution was 65, 70 and 72% at 50, 100 and 150 µg/ml concentrations of PFE, respectively. This observation is important as the regulation of cell cycle is crucial in the growth and development of cancer and currently, cell cycle is targeted for intervention against cancer.

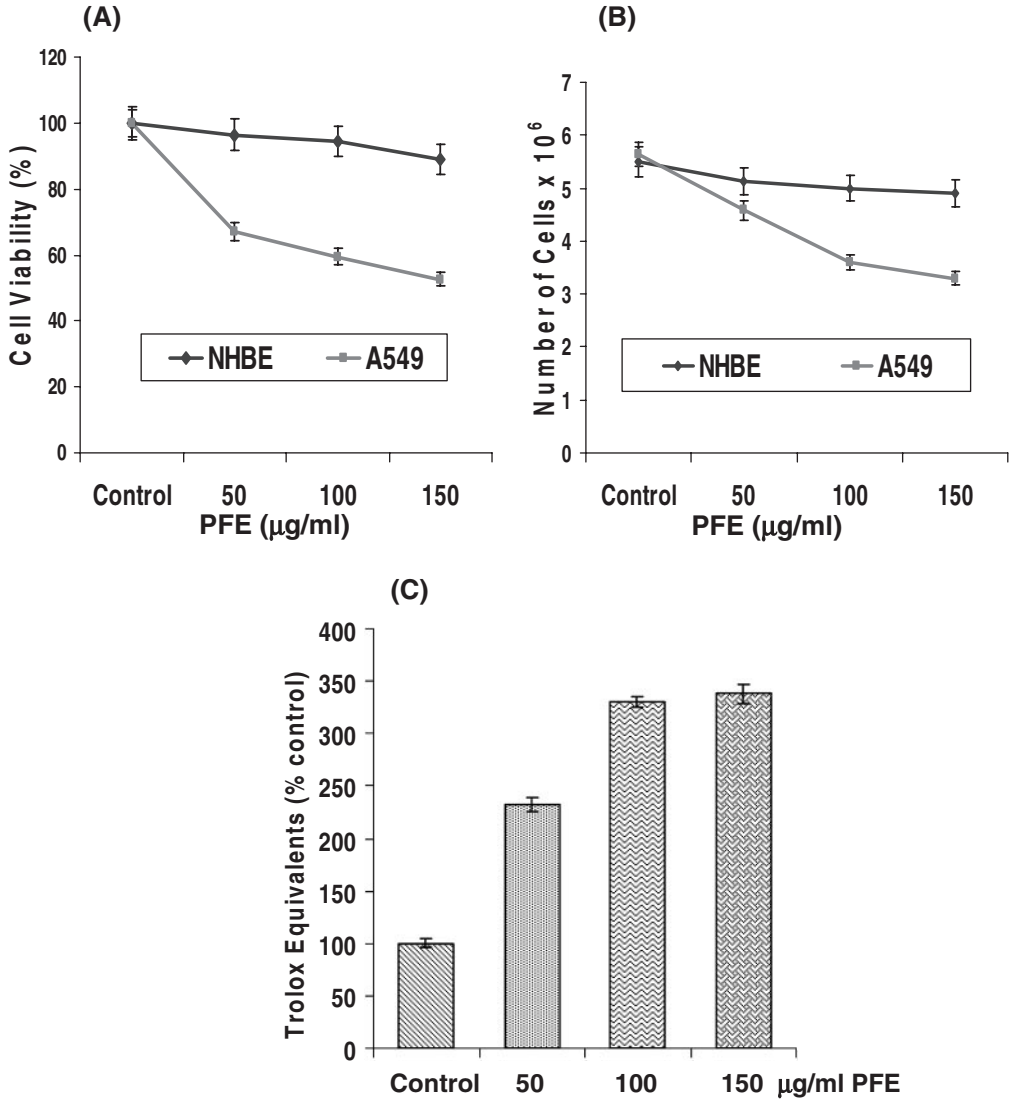

Fig. 1. (**A**) Effect of PFE on cell growth. As detailed in Materials and methods, A549 and NHBE cells were treated with PFE and the viability of cells was determined by the MTT assay. The data are expressed as the percentage of cell viability and represent the means ± SE of three experiments in which each treatment was performed in multiple wells. (**B**) Cell growth inhibition by Trypan blue exclusion assay. (**C**) Antioxidant capacity of PFE in A549 cells. Assessment of antioxidant activity of PFE in A549 cells was done by trolox antioxidant assay as described in Materials and methods.

Induction of WAF1/p21, KIP1/p27 and consequent inhibition of cyclins D1, D2 and E and cdk2, cdk4 and cdk6 by PFE in A549 cells

As our study demonstrated that PFE treatment of A549 cells resulted in G_1 phase cell cycle arrest, we examined the effect of PFE on cell cycle-regulatory molecules operative in the G_1 phase of the cell cycle. We assessed the effect of PFE on the induction of WAF1/p21 and KIP1/p27 which are known to regulate the entry of cells at the G_1–S phase transition checkpoint. Immunoblot analysis revealed that PFE treatment of the cells resulted in a marked induction of WAF1/p21 and KIP1/p27 in a dose-dependent manner compared with the basal levels (Figure 3A). Using immunoblot analysis, we also assessed the effect of PFE treatment on the protein expressions of the cyclins and cdks, which are known to be regulated by WAF1/p21. PFE treatment of the cells resulted in a dose-dependent decrease in protein expressions of cyclin D1, cyclin D2 and cyclin E (Figure 3B) as well as cdk 2, cdk4 and cdk6 (Figure 3C).

Inhibition of NF-κB and IKKα and phosphorylation and degradation of IκBα by PFE in A549 cells

It has been documented that one of the critical events in NF-κB activation is its dissociation with subsequent degradation of inhibitory protein IκBα via phosphorylation and ubiquitination. The treatment of A549 cells with PFE (50–150 μg/ml) resulted in a significant inhibition in the phosphorylation of IκBα protein. Western blot analysis and relative density of the bands showed that the phosphorylation of IκBα protein was almost completely inhibited at 150 μg/ml of PFE (Figure 4A). To evaluate the possible inhibitory mechanism of PFE on IκBα protein degradation, we measured IKKα protein level. Western blot analysis showed that pretreatment of A549 cells with PFE inhibits IKKα in a dose-dependent manner (Figure 4A).

We investigated whether treatment with PFE (50–150 μg/ml) inhibits nuclear translocation of NF-κB/p65 in A549 cells. As is evident from western blot analysis data and the relative density of bands, we found that PFE treatment

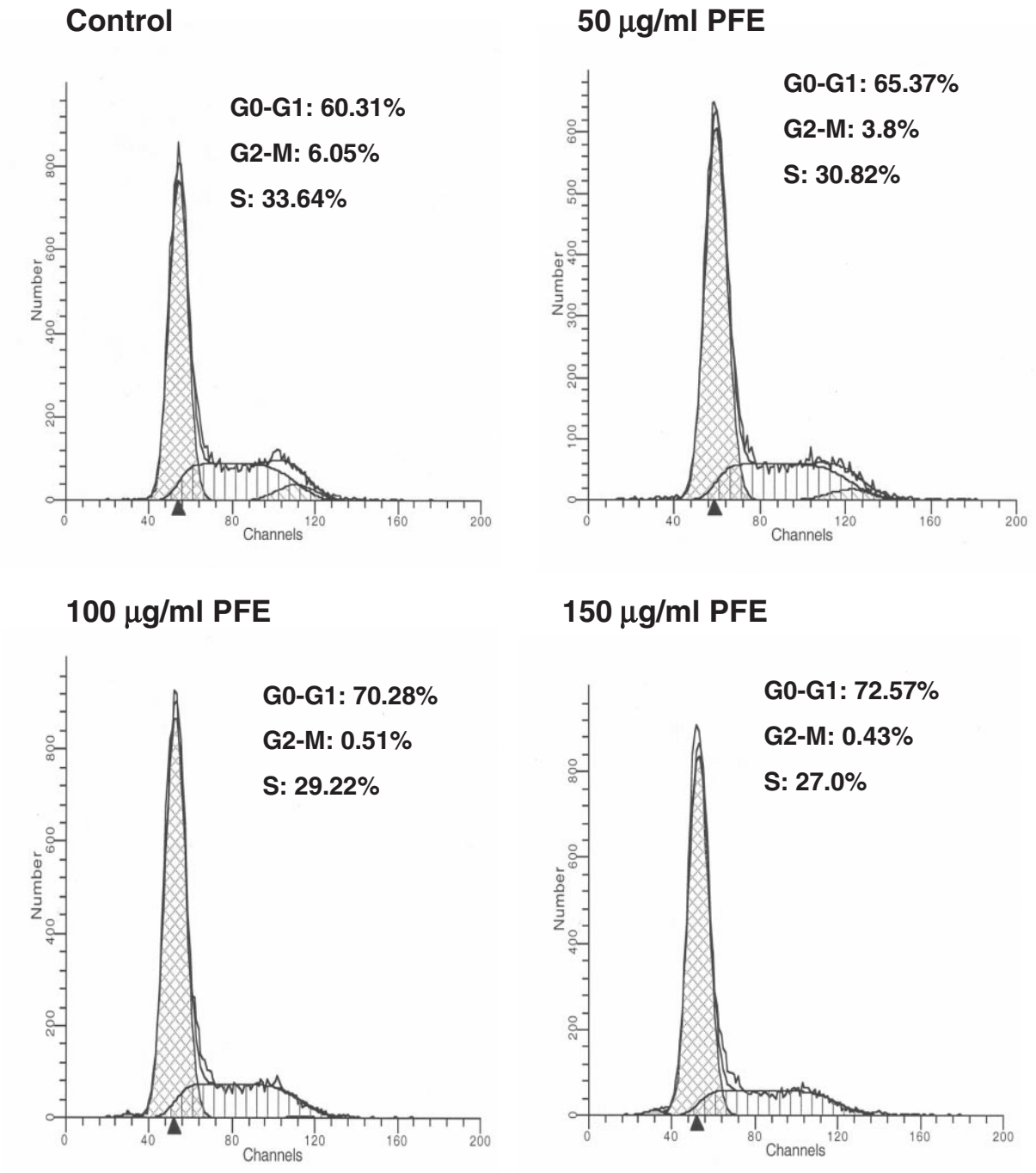

Fig. 2. Effect of PFE on cell cycle distribution in A549 cells. The cells treated with PFE were collected and stained with PI by using an apoptosis APO-DIRECT kit obtained from Phoenix Flow systems as per vendor's protocol followed by flow cytometry. Following FACS analysis, cellular DNA histograms were further analyzed by ModfitLT V3.0. The data are representative example for duplicate tests. The details are described in Materials and methods.

of A549 cells resulted in inhibition of translocation of NF-κB/p65 (Figure 4B). We further confirmed our results by performing EMSA and enzyme-linked immunosorbent assay (ELISA). Employing ELISA, we found that pretreatment of A549 cells with PFE (50–150 μg/ml) significantly inhibited nuclear translocation of NF-κB/p65 (Figure 4C). As shown by EMSA in Figure 4D, PFE treatment inhibited NF-κB DNA-binding activity in A549 cells. Immunocytochemical staining of A549 cells further confirmed this effect. In PFE-treated cells, slight cytoplasmic immunostaining was seen with anti-p65 antibody whereas control cells showed an intense nuclear fluorescence (Figure 4E) signifying an inhibitory effect of PFE on the translocation of the NF-κB/p65 subunits into the nuclei.

Inhibition of phosphorylation of MAPKs by PFE in A549 cells

The MAP kinase superfamily has been characterized into three groups which include extracellular signal-regulated kinase p44/42 (ERK), JNK/SAPK (c-jun N-terminal kinase/stress activated protein kinase) and p38 MAP kinase. To determine the effect of PFE (50–150 μg/ml) on phosphorylation of MAPKs in A549 human lung carcinoma cells,

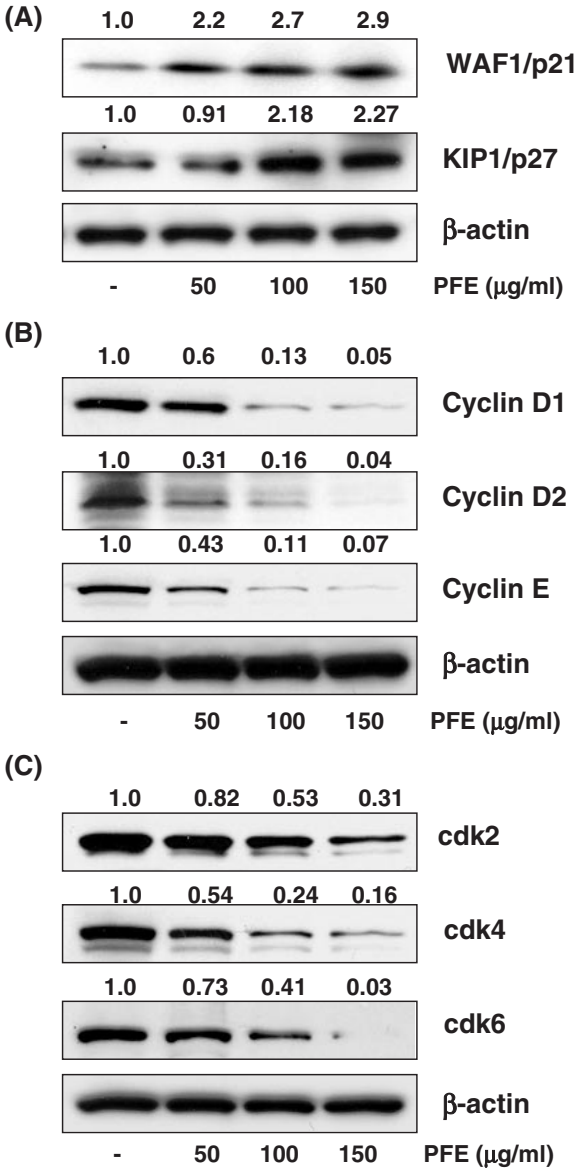

Fig. 3. (**A**) Effect of PFE on protein expression of WAF1/p21 and KIP1/p27 in human lung carcinoma A549 cells. (**B**) Effect of PFE on protein expression of cyclin D1, cyclin D2 and E in human lung carcinoma A549 cells. (**C**) Effect of PFE on protein expression of cdk2, cdk4 and cdk6 in human lung carcinoma A549 cells. As detailed in Materials and methods, the cells were treated with PFE (50–150 μg/ml) and then harvested. Total cell lysates were prepared and 40 μg protein was subjected to SDS–PAGE followed by immunoblot analysis and chemiluminescence detection. Equal loading of protein was confirmed by stripping the immunoblot and reprobing it for β-actin. The immunoblots shown here are representative of three independent experiments with similar results. The values above the figures represent relative density of the bands normalized to β-actin.

western blot analysis was performed using phospho-specific MAPKs antibodies. In the present study, as evident from western blot analysis, we found that PFE (50–150 μg/ml) resulted in a decrease in phosphorylation of ERK1/2 (p44 and p42), JNK1/2 (p54 and p46) and p38 proteins in A549 human lung carcinoma cells (Figure 5A).

Inhibition of PI3K and phosphorylation of Akt protein expression by PFE in A549 cells

Studies have shown that PI3K plays an important role in carcinogenesis. We first investigated the effect of PFE on PI3K protein expression in A549 human lung carcinoma cells. Western blot analysis and the relative density of bands revealed that PFE caused inhibition in the expression of both regulatory (p85) as well as catalytic (p110) subunits of PI3K in A549 human lung carcinoma cells (Figure 5B).

Akt, also known as protein kinase B, which is a serine or threonine kinase, has been identified as an important component of prosurvival signaling pathway. In human lung carcinoma A549 cells, PFE (50–150 μg/ml) inhibited phosphorylation of Akt at Thr^{308} (Figure 5B).

Inhibition of cell proliferation markers-Ki-67 and proliferating cell nuclear antigen by PFE in A549 cells

The decrease in the growth and viability of A549 cells by PFE treatment could be attributed to the antiproliferative effects of PFE. Therefore, we evaluated the effect of PFE treatment of A549 cells on the levels of Ki-67 and proliferating cell nuclear antigen (PCNA), which are the cell proliferation markers. As shown by immunocytochemical analysis in Figure 6A, intense Ki-67 staining is evident in control group. Treatment with PFE (50–150 μg/ml) resulted in marked reduction in the Ki-67 protein expression. PFE treatment also caused the reduction in the PCNA protein expression as shown by western blot analysis and the relative density of bands (Figure 6B).

Inhibition on the growth of human lung carcinoma A549 cells by PFE in nude mice

The treatment of nude mice with PFE given as the sole source of drinking fluid resulted in inhibition of A549 tumor xenograft growth. The appearance of small solid tumors was observed in animals receiving water as drinking fluid 15 days after cell inoculation. This latency period was prolonged to 19 days in animals receiving PFE in drinking fluid. PFE (0.1 and 0.2%) was administered orally *ad libitum* to these animals Day 1 after tumor cell implantation. As shown in Figure 7A, tumor growth, as inferred by computed tumor volume, was significantly inhibited in mice receiving both 0.1 and 0.2% PFE with higher inhibitory effects observed in animals receiving 0.2% PFE than in those receiving 0.1% PFE. In this protocol, we killed the animals when the tumor reached a volume of 1200 mm^3. In control group, the average tumor volume of 1200 mm^3 was reached in 55 ± 2 days after tumor cell inoculation. At this time point, the average tumor volumes of the 0.1 and 0.2% PFE-fed groups were 621 and 540 mm^3, respectively. The average tumor volume of 1200 mm^3 was achieved in 67 ± 4 days after tumor cell inoculation in 0.1% PFE-fed group. The 0.2% PFE-fed group showed the most effective tumor growth inhibitory response with the targeted average tumor volume of 1200 mm^3 was reached at 79 ± 3 days after tumor cell inoculation (Figure 7B). Tumor data were analyzed for survival probability by Kaplan–Meier analysis, which indicated that continuous PFE infusion to athymic nude mice resulted in increased survival ($P < 0.0001$, log-rank test), with a median survival of 67 and 79 days (0.1 and 0.2% PFE, respectively), compared with 55 days in water-fed mice ($P < 0.0001$, log-rank test) (data not shown).

Discussion

Lung cancer has the highest US and worldwide rate of cancer mortality, exceeding the mortality rates of colorectal, breast

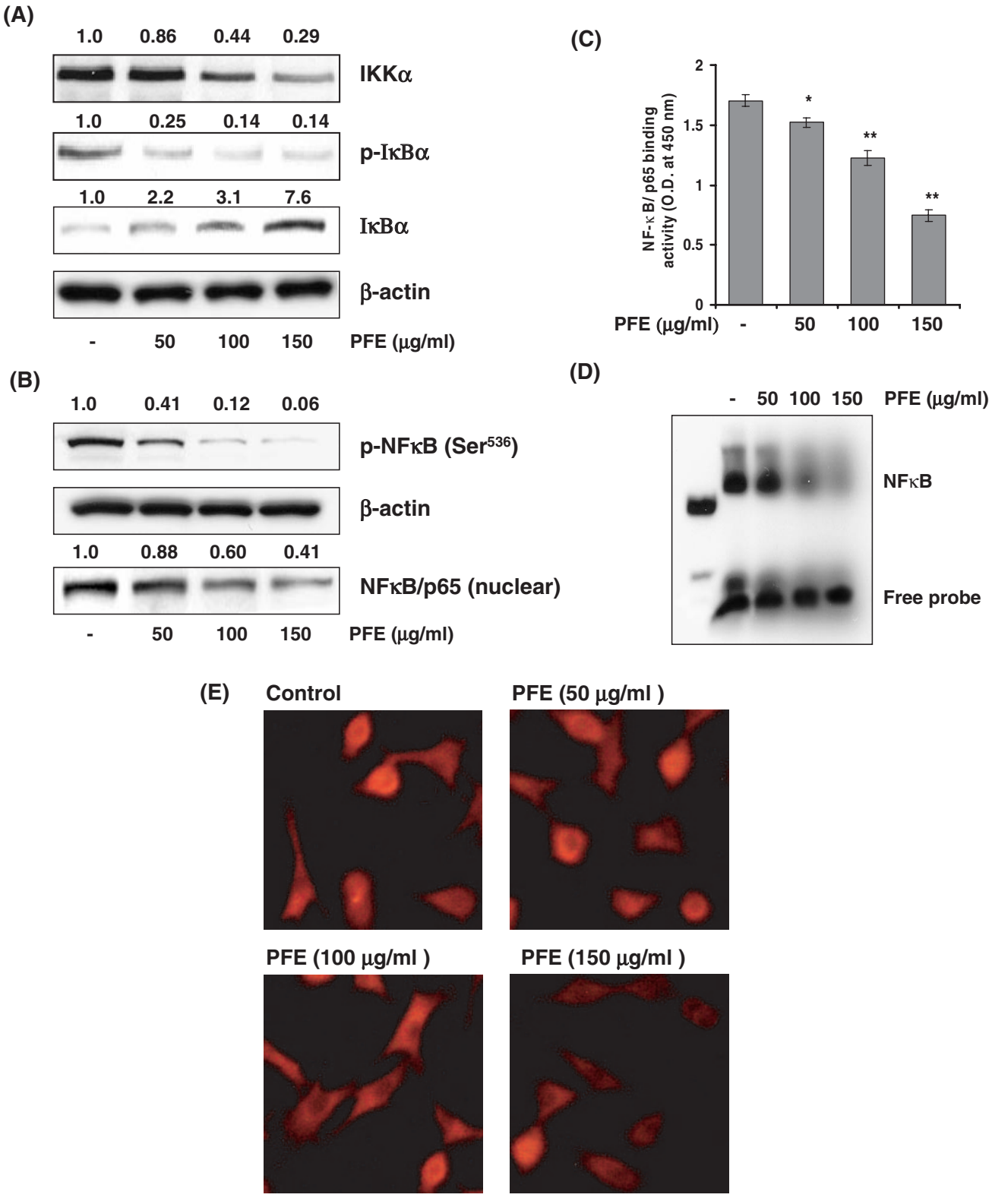

Fig. 4. (**A**) Effect of PFE on IKKα and phosphorylation and degradation of IκBα in human lung carcinoma A549 cells. (**B**) Effect of PFE on activation of NFκB in human lung carcinoma A549 cells by western blot analysis. As detailed in Materials and methods, the cells were treated with PFE (50–150 μg/ml) and then harvested and nuclear lysate was prepared and protein was subjected to SDS–PAGE followed by immunoblot analysis and chemiluminescence detection. Equal loading of protein was confirmed by stripping the immunoblot and reprobing it for β-actin. The immunoblots shown here are representative of three independent experiments with similar results. The values above the figures represent relative density of the bands normalized to β-actin. (**C**) EMSA and (**D**) ELISA for the NFκB binding complex was demonstrated by anti-p65 antibody. (**E**) A549 cells were seeded in tissue culture glass slides and treated with PFE (50–150 μg/ml). Briefly, cells were fixed in 2% paraformaldehyde and incubated with NF-κB/p65 antibody followed by incubation with donkey anti-rabbit Rhodamine Red TM-X-conjugated antibody. Samples were mounted using Prolong antifade kit and observed using a Zeiss Axiophot DM HT microscope. The data shown here are from one representative experiment repeated two times with similar results.

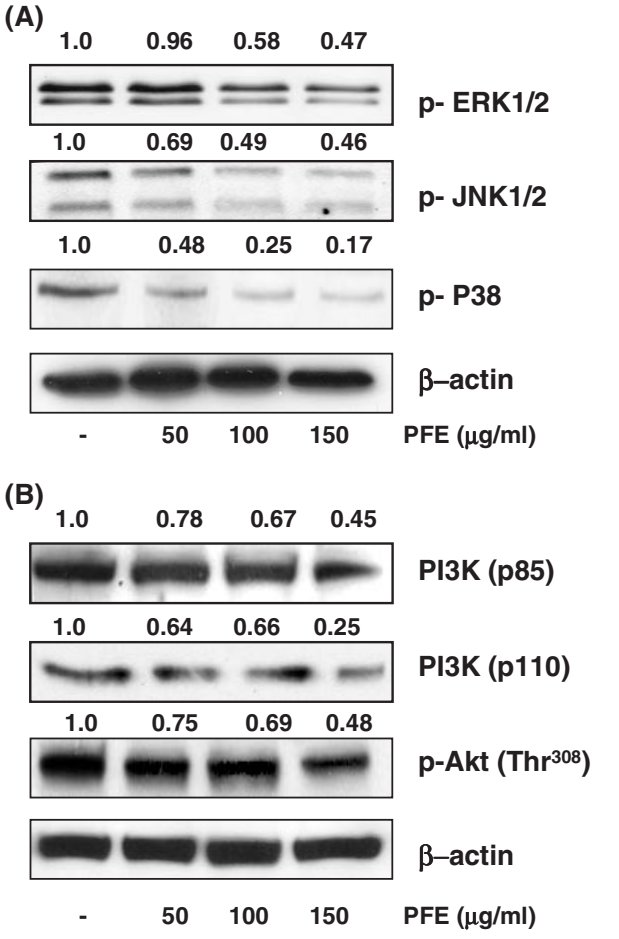

Fig. 5. (**A**) Inhibitory effects of PFE on phosphorylation of MAPKs (ERK, JNK and P38) in human lung carcinoma A549 cells. (**B**) Inhibitory effects of PFE on PI3K (p85 and p110 and phosphorylation of Akt (Thr^{308}) in human lung carcinoma A549 cells. As detailed in Materials and methods, the cells were treated with PFE (50–150 μg/ml) and then harvested. Whole cell lysate was prepared and 40 μg protein was subjected to SDS–PAGE followed by immunoblot analysis and chemiluminescence detection. Equal loading of protein was confirmed by stripping the immunoblot and reprobing it for β-actin. The immunoblots shown here are representative of three independent experiments with similar results. The values above the figures represent relative density of the bands normalized to β-actin.

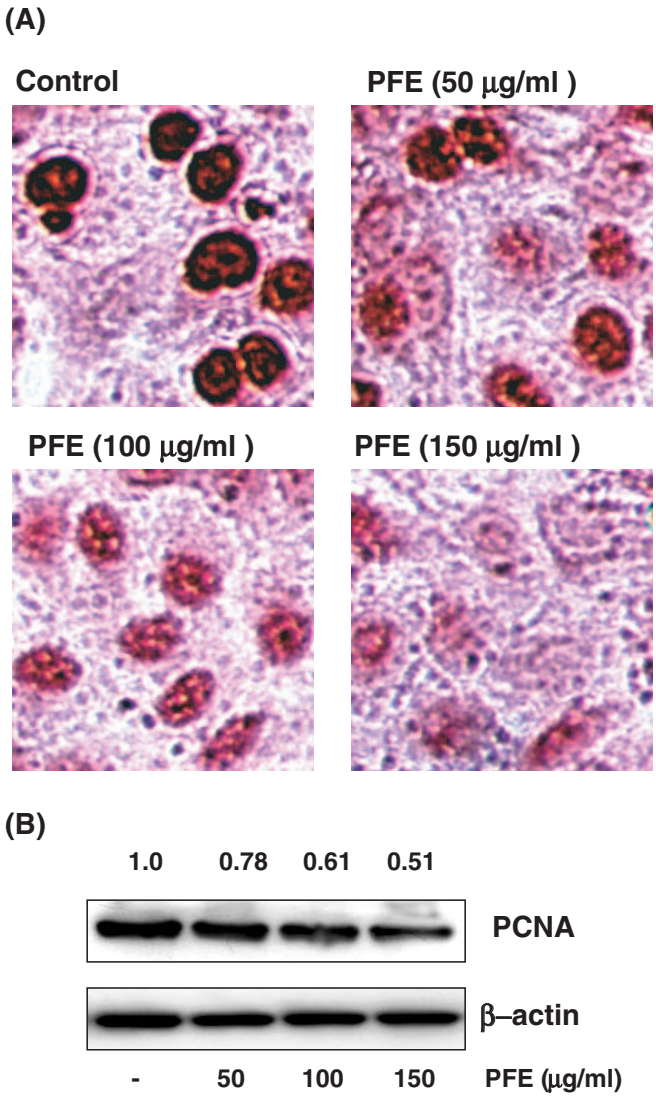

Fig. 6. (**A**) Immunostaining of Ki-67. A549 cells were grown in tissue culture slides and treated with PFE (50–150 μg/ml) for 72 h. The cells were stained for Ki-67 as detailed in Materials and methods. A brown color indicates the presence of Ki-67 protein in the nuclei of cells. Counterstaining was performed with eosin, ×400. The data shown here are from one representative experiment repeated two times with similar results. (**B**) Effect of PFE on protein expression of PCNA in human lung carcinoma A549 cells. As detailed in Materials and methods, the cells were treated with PFE (50–150 μg/ml) and then harvested. Total cell lysates were prepared and 40 μg protein was subjected to SDS–PAGE followed by immunoblot analysis and chemiluminescence detection. Equal loading of protein was confirmed by stripping the immunoblot and reprobing it for β-actin. The immunoblots shown here are representative of three independent experiments with similar results. The values above the figures represent relative density of the bands normalized to β-actin.

and prostate cancers combined (13). Cigarette smoking is the single largest cause of lung cancer and smoking cessation, therapy and screening have limited success in controlling lung cancer incidence, morbidity and mortality which have not improved substantially in decades. The heavy burden of lung cancer and its resistance to standard approaches (smoking cessation, screening and therapy) have motivated an intense interest in the promising approach of chemoprevention for controlling this disease (14). Lung carcinogenesis is a chronic and multistep process resulting in malignant lung tumors. This progression from normal to neoplastic pulmonary cells or tissues could be arrested or reversed through pharmacological treatments. These therapeutic interventions should reduce or avoid the clinical consequences of lung cancer by treating early neoplastic lesions before the development of clinically evident signs or symptoms of malignancy. Preclinical, clinical and epidemiological findings relating to different classes of candidate chemopreventive agents provide strong support for lung cancer prevention as a therapeutic strategy (15). Cancer chemoprevention is an attractive approach to reduce lung cancers by treating early steps in lung carcinogenesis. There is a convergence of basic scientific and clinical findings in lung cancer chemoprevention. Pharmacological interventions also can be used to reverse or arrest the progression of lung carcinogenesis. While promising pharmacological evidence exists for lung cancer chemoprevention, the optimal agent has not yet been identified that is active in primary or secondary lung cancer chemoprevention. For this reason, additional clinical trials

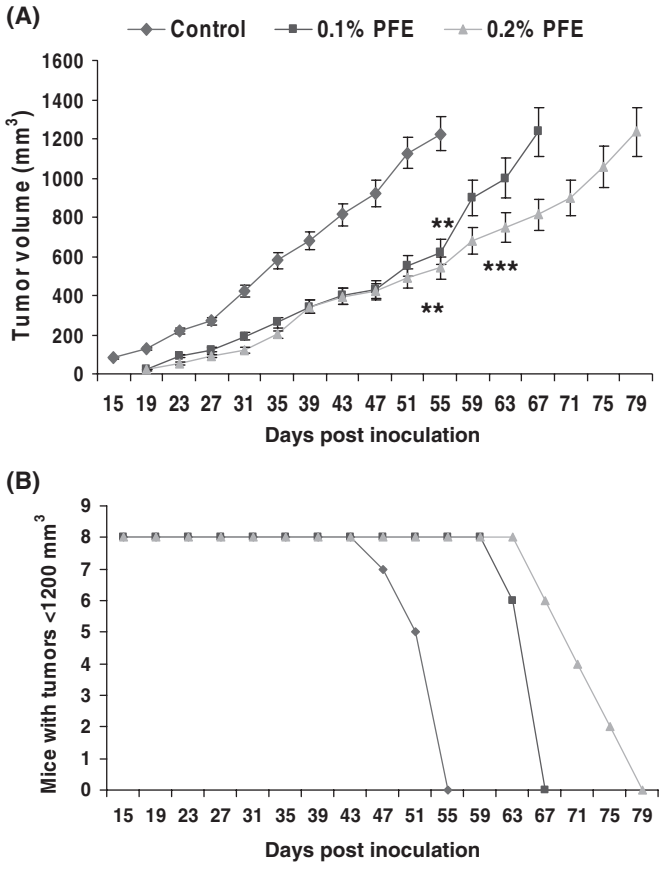

Fig. 7. Effect of oral administration of PFE on A549 tumor growth in athymic nude mice. Approximately 1 million A549 cells were s.c. injected in each flank of the mouse to initiate tumor growth. Twenty-four hours after cell implantation, the control group of animals continued to receive sterilized drinking water whereas animals of Groups 2 and 3 received 0.1 and 0.2% PFE, respectively, in the same drinking water *ad libitum.* Water bottles were changed every other day. Once tumors started to grow, their sizes were measured twice weekly and the tumor volume was calculated. (**A**) Average tumor volume of water-fed, 0.1 and 0.2% PFE-fed mice plotted over days after tumor cell inoculation. (**B**) Number of mice remaining with tumor volumes $\leq$1200 mm^3 after they consumed 0.1 and 0.2% PFE for the indicated days. Values represent mean ± SE of eight animals. *$P < 0.01$, **$P < 0.001$ versus the water-fed group of mice; ***$P < 0.01$ versus the 0.1% PFE-fed group of mice. Details are described in Materials and methods.

are needed that emphasize a mechanistic approach in which mechanisms identified *in vitro* can be validated *in vivo*.

This study was designed to show the chemopreventive/chemotherapeutic potential of PFE against lung cancer. Treatment of A549 cells with PFE resulted in decrease in cell viability but had minimal effect on NHBE cells (Figure 1A). The dose-dependent growth inhibitory effect on A549 cells was also confirmed by Trypan blue exclusion assay (Figure 1B). PFE was also found to have high antioxidant activity when measured by trolox assay (Figure 1C). PFE treatment of A549 cells also resulted in dose-dependent arrest of cells in G_1 phase of the cell cycle (as assessed by DNA cell cycle analysis, Figure 2). However, as assessed by TUNEL (terminal deoxynucleotide transferase dUTP nick-end labeling) assay for labeling DNA breaks and total cellular DNA to detect apoptotic cells by flow cytometry, PFE treatment did not induced apoptosis in A549 cells (data not shown).

To define the mechanism of antiproliferative effects of PFE against lung cancer, we investigated the involvement of cyclin kinase inhibitor–cyclin–cyclin-dependent kinase machinery during the induction of cell cycle arrest by PFE in A549 cells. Abnormal expression of cell cycle-regulatory molecules may cause alterations in cell cycle resulting in an uncontrolled cell growth, a universal feature of neoplasia. Proliferation in mammalian cells is primarily achieved in the G_1 phase of the cell cycle through the action of the G_1 cyclins and their regulatory cyclin-dependent kinases (cdks). After G_1 phase, the cells become largely independent of extracellular signals and progress automatically through subsequent cell cycle to the next G_1 phase (16). Cdk activities are regulated by a group of specific inhibitory proteins known as cyclin-dependent kinase inhibitors (cdkis). In controlled cell growth, association of cyclins D and E with cdk 2, 4 or 6 leads to phosphorylation of retinoblastoma protein (pRb), hyperphosphorylated pRb (ppRb) leads to its release from E2F and the cell exits the G_1 phase. The free E2F then activates transcription of genes required for progression through the S phase, thus driving the transition from G_1 to S phase. Any defect in this machinery causes an altered cell cycle regulation that may result in unwanted cellular proliferation ultimately culminating in the development of cancer (17,18). Thus, we examined the effect of PFE on cell cycle-regulatory molecules operative in the G_1 phase of the cell cycle. Our data demonstrated a significant upregulation of the cki WAF1/p21 and KIP1/p27 by PFE (Figure 3A). Since, WAF1/p21 and KIP1/p27 are considered as universal inhibitor of cyclin–cdk complexes, we therefore assessed the effect of PFE treatment on the cyclins and cdks operative in the G_1 phase of the cell cycle, i.e. cyclins D1, D2 and E and cdks 2, 4 and 6. We found that PFE treatment of the cells resulted in significant downregulation of all of these regulatory molecules (Figure 3A–C).

NF-κB is a sequence specific transcription factor that is known to be involved in the inflammatory and innate immune responses (19,20). NF-κB is sequestered in the cytoplasm in an inactive form through interaction with IκB. Phosphorylation of IκB by IκB kinase (IKK) causes ubiquitination and degradation of IκB, thus releasing NF-κB which then translocates to the nucleus, where it binds to specific κB binding sites in the promoter regions of several genes (21). Studies have shown that NF-κB activation plays an important role in cell survival, by its ability to block or reduce apoptosis (22). In the present study, we further investigated the effect of PFE on the pattern of NF-κB activation and its nuclear translocation in A549 human lung carcinoma cells. We found that NF-κB is activated in A549 human lung carcinoma cells and is translocated to the nucleus when measured by western blot analysis, ELISA, EMSA and immunocytochemical analysis (Figure 4A–E). The IKK complex is believed to be an important site for integrating signals that regulate the NF-κB pathway. Our results showed a positive correlation between NF-κB/p65 activation and its translocation to the nucleus and phosphorylation and degradation of IκBα in the cytoplasm. Interestingly, we found that treatment of PFE in A549 human lung carcinoma cells significantly inhibited IKKα and phosphorylation and degradation of IκBα protein (Figure 4A). As PFE blocks IκBα phosphorylation and degradation, this study suggests that the effects of PFE on NF-κB/p65 are through inhibition of phosphorylation and subsequent proteolysis of IκBα. It is well documented that through a protein–protein interaction, IκBα is bound to NF-κB/p65 and thus prevents migration of NF-κB/p65 into the nucleus (21,23).

MAPKs, a group of serine/threonine-specific, proline-directed protein kinases are known to modulate transcription factor activities. (24,25). The involvement of the MAPK pathway in tumor proliferation is well documented. Transient activation of ERK is responsible for proliferation and differentiation and has also been shown to be involved in tumor promotion processes (26). Stimulation of JNK/SAPK and p38 can mediate differentiation, inflammatory responses and cell death (27). In the present study, we assessed the effect of PFE on phosphorylation of MAPK pathway in A549 human lung carcinoma cells. The immunoblot analysis demonstrated that the treatment of cells with PFE inhibited phosphorylation of ERKl/2, JNK1/2 and p38 proteins (Figure 5A). Several studies have shown that JNK pathway plays a major role in cellular function, such as cell proliferation and transformation, whereas the ERK pathway suppresses apoptosis and enhances cell survival or tumorigenesis (24). ERK1/2 and p38 are also involved in the transcriptional activation of NF-κB (28,29).

PI3K is another important effector of the erbB RTKs. It appears to play a critical role in cell survival rather that cell proliferation (26). When PI3K is activated by these receptor tyrosine kinases, it synthesizes the second messenger phosphatidylinositol triphosphate, which is necessary for recruitment to the membrane fraction and phosphorylation of the serine/threonine kinase Akt. Indeed, the strong prosurvival signaling mediated by PI3K is largely due to its ability to activate Akt (30). In our study, we have demonstrated that the treatment of A549 cells with PFE resulted in reduction in the expression of PI3K (p85 and p110) and phosphorylation of Akt at Thr^{308} (Figure 5B). As Akt is a downstream substrate for PI3K and phosphorylation form of Akt is a prerequisite for the catalytic activity of Akt. The PI3K/Akt promotes cell survival by activating the NF-κB signaling pathway (26). We evaluated the effect of PFE on the levels of Ki-67 and PCNA, which are the cell proliferation markers expressed by actively proliferating cells and rapidly degrade as the cell enters the non-proliferative stage. We found that on treatment with PFE there was marked reduction in the levels of Ki-67 and PCNA as evident by immunocytochemical analysis and western blotting (Figure 6A and B, respectively).

To establish the relevance of these *in vitro* findings to *in vivo* situation, athymic nude mice were implanted with human lung carcinoma A549 cells. We found that the oral administration of PFE significantly slowed the progression of A549 tumor growth in nude mice (Figure 7A and B). Based on the present study it is tempting to suggest that PFE and its associated antioxidants have strong potential for development as a chemopreventive and possibly as a chemotherapeutic agent against lung cancer. Thus, these could be important observations that may be useful for devising strategies for the management of lung cancer. In depth studies with PFE in animal models of lung cancer are warranted. In conclusion, the present study demonstrates that human non-small cell lung cancer A549 cells are highly sensitive to growth inhibition by PFE both in *in vitro* and *in vivo* experimental models. PFE inhibits the development of lung tumorigenesis by G_1 phase cell cycle arrest, modulating *cki-cyclin-cdk* network and inhibiting MAPK, NFκB and PI3K/Akt signaling. These findings suggest that PFE may be a promising chemopreventive/chemotherapeutic agent against human non-small cell lung cancer.

Acknowledgements

This study was supported by the developmental funds from US Public Health Service Grant 5P30 CA 14520 and also used resources of USPHS grants R01 CA 78809 and R01 CA 101039.

Conflict of Interest Statement: None declared.

References

1. Parkin,D.M., Bray,F., Ferlay,J. and Pisani,P. (2001) Estimating the world lung cancer burden: Globocan 2000. *Int. J. Cancer*, **94**, 153–156.
2. Doll,R. and Peto,R. (1981) The causes of cancer: quantitative estimates of avoidable risks of cancer in the United States today. *J. Natl Cancer Inst.*, **66**, 1191–1308.
3. Jemal,A., Siegel,R., Ward,E., Murray,T., Xu,J., Smigal,C. and Thun,M.J. (2006) Cancer statistics, 2006. *CA Cancer J Clin.*, **56**, 106–130.
4. de Nigris,F., Williams-Ignarro,S., Botti,C., Sica,V., Ignarro,L.J. and Napoli,C. (2006) Pomegranate juice reduces oxidized low-density lipoprotein downregulation of endothelial nitric oxide synthase in human coronary endothelial cells. *Nitric Oxide* (Epub ahead of print).
5. de Nigris,F., Williams-Ignarro,S., Lerman,L.O. *et al.* (2005) Beneficial effects of pomegranate juice on oxidation-sensitive genes and endothelial nitric oxide synthase activity at sites of perturbed shear stress. *Proc. Natl Acad. Sci. USA*, **102**, 4896–4901.
6. Schubert,S.Y., Neeman,I. and Resnick,N. (2002) A novel mechanism for the inhibition of NF-κB activation in vascular endothelial cells by natural antioxidants. *FASEB J.*, **16**, 1931–1933.
7. Gil,M.I., Tomas-Barberan,F.A., Hess-Pierce,B., Holcroft,D.M. and Kedar,A.A. (2000) Antioxidant activity of pomegranate juice and its relationship with phenolic composition and processing. *J. Agric. Food Chem.*, **10**, 4581–4589.
8. Afaq,F., Saleem,M., Krueger,C.G., Reed,J.D. and Mukhtar,H. (2005) Anthocyanin and hydrolyzable tannin-rich pomegranate fruit extract modulates MAPK and NF-kappaB pathways and inhibits skin tumorigenesis in CD-1 mice. *Int. J. Cancer*, **113**, 423–433.
9. Malik,A., Afaq,F., Sarfaraz,S., Adhami,V.M., Syed,D.N. and Mukhtar,H. (2005) Pomegranate fruit juice for chemoprevention and chemotherapy of prostate cancer. *Proc. Natl Acad. Sci. USA*, **102**, 14813–14818.
10. Afaq,F., Malik,A., Syed,D., Maes,D., Matsui,M.S. and Mukhtar,H. (2005) Pomegranate fruit extract modulates UV-B-mediated phosphorylation of mitogen-activated protein kinases and activation of nuclear factor kappa B in normal human epidermal keratinocytes paragraph sign. *Photochem. Photobiol.*, **81**, 38–45.
11. Syed,D.N., Malik,A., Hadi,N., Sarfaraz,S., Afaq,F. and Mukhtar,H. (2006) Photochemopreventive effect of pomegranate fruit extract on UVA-mediated activation of cellular pathways in normal human epidermal keratinocytes. *Photochem. Photobiol.*, **82**, 398–405.
12. Tomayko,M.M. and Reynolds,C.P. (1989) Determination of subcutaneous tumor size in athymic (nude) mice. *Cancer Chemother. Pharmacol.*, **24**, 148–154.
13. Parkin,D.M., Bray,F., Ferlay,J. and Pisani,P. (2005) Global cancer statistics, 2002. *CA Cancer J. Clin.*, **55**, 74–108.
14. Peto,R., Darby,S., Deo,H., Silcocks,P., Whitley,E. and Doll,R. (2000) Smoking, smoking cessation and lung cancer in the UK since 1950: combination of national statistics with two case-control studies. *Br. Med. J.*, **321**, 323–329.
15. Cohen,V. and Khuri,F.R. (2002) Chemoprevention of lung cancer: current status and future prospects. *Cancer Metastasis Rev.*, **21**, 349–362.
16. Ahmad,N., Feyes,D.K., Agarwal,R. and Mukhtar,H. (1998) Photodynamic therapy results in induction of WAF1/CIP1/P21 leading to cell cycle arrest and apoptosis. *Proc. Natl Acad. Sci. USA*, **95**, 6977–6982.
17. Sanchez,I. and Dynlacht,B.D. (2005) New insights into cyclins, CDKs and cell cycle control. *Semin. Cell Dev. Biol.*, **16**, 311–321.
18. Jacks,T. and Weinberg,R.A. (1996) Cell-cycle control and its watchman. *Nature*, **381**, 643–644.
19. Baldwin,A.S. Jr. (1996) The NF-kappa B and I kappa B proteins: new discoveries and insights. *Annu. Rev. Immunol.*, **14**, 649–683.
20. Maniatis,T. (1997) Catalysis by a multiprotein IkappaB kinase complex. *Science*, **278**, 818–819.
21. Gupta,S., Hastak,K., Afaq,F., Ahmad,N. and Mukhtar,H. (2004) Essential role of caspases in epigallocatechin-3-gallate-mediated inhibition of nuclear factor kappa B and induction of apoptosis. *Oncogene*, **23**, 2507–2522.
22. Kaufman,C.K. and Fuchs,E. (2000) It's got you covered. NF-kappaB in the epidermis. *J. Cell Biol.*, **149**, 999–1004.

23. Baeuerle,P.A. and Baltimore,D. (1996) NF-kappa B: ten years after. *Cell*, **87**, 13–20.
24. Afaq,F., Ahmad,N. and Mukhtar,H. (2003) Suppression of UVB-induced phosphorylation of mitogen-activated protein kinases and nuclear factor kappa B by green tea polyphenol in SKH-1 hairless mice. *Oncogene*, **22**, 9254–9264.
25. Katiyar,S.K., Afaq,F., Azizuddin,K. and Mukhtar,H. (2001) Inhibition of UVB-induced oxidative stress-mediated phosphorylation of mitogen-activated protein kinase signaling pathways in cultured human epidermal keratinocytes by green tea polyphenol (−)-epigallocatechin-3-gallate. *Toxicol. Appl. Pharmacol.*, **176**, 110–117.
26. Adhami,V.M., Siddiqui,I.A., Ahmad,N., Gupta,S. and Mukhtar,H. (2004) Oral consumption of green tea polyphenols inhibits insulin-like growth factor-I-induced signaling in an autochthonous mouse model of prostate cancer. *Cancer Res.*, **64**, 8715–8722.
27. Cobb,M.H. and Goldsmith,E.J. (1995) How MAP kinases are regulated. *J. Biol. Chem.*, **270**, 14843–14846.
28. Adderley,S.R. and Fitzgerald,D.J. (1999) Oxidative damage of cardiomyocytes is limited by extracellular regulated kinases 1/2-mediated induction of cyclooxygenase-2. *J. Biol. Chem.*, **274**, 5038–5046.
29. Carter,A.B., Knudtson,K.L., Monick,M.M. and Hunninghake,G.W. (1999) The p38 mitogen-activated protein kinase is required for NF-kappaB-dependent gene expression: the role of TATA-binding protein (TBP). *J. Biol. Chem.*, **274**, 30858–30863.
30. Stambolic,V., Mak,T.W. and Woodgett,J.R. (1999) Modulation of cellular apoptotic potential: contributions to oncogenesis. *Oncogene*, **18**, 6094–6103.

Received May 18, 2006; revised July 24, 2006; accepted August 4, 2006